0026-895X/05/6706-1892–1900$20.00
MOLECULAR PHARMACOLOGY
Copyright © 2005 The American Society for Pharmacology and Experimental Therapeutics
Mol Pharmacol 67:1892–1900, 2005

Vol. 67, No. 6
12179/3035053
Printed in U.S.A.

Differential Spatial Approximation between Cholecystokinin Residue 30 and Receptor Residues in Active and Inactive Conformations

Maoqing Dong, Elizabeth M. Hadac, Delia I. Pinon, and Laurence J. Miller
Mayo Clinic Cancer Center and Department of Molecular Pharmacology and Experimental Therapeutics, Scottsdale, Arizona

Received February 21, 2005; accepted March 17, 2005

ABSTRACT

Understanding the structures of active and inactive agonist- and antagonist-bound receptor complexes is of great interest. In this work, we focus on position 30 of cholecystokinin (CCK) and its spatial approximation with the type A CCK receptor. For this, we developed two photoaffinity labeling probes, replacing the naturally occurring tryptophan with *p*-benzoyl-L-phenylalanine (Bpa) or *p*-nitro-phenylalanine (NO_2-Phe). The Bpa probe was shown to represent an antagonist, whereas the NO_2-Phe probe stimulated intracellular calcium as a fully efficacious agonist (EC_{50} = 81 ± 15 nM). Both ligands bound to the receptor specifically, although with lower affinity than CCK (K_i values: Bpa probe, 270 ± 72 nM; NO_2-Phe probe, 180 ± 40 nM). Both probes covalently labeled the receptor in an efficient manner. The Bpa antagonist labeled the receptor in two distinct regions as identified by cyanogen bromide cleavage, with labeled bands migrating at M_r = 25,000 and 4500. The former represented the glycosylated amino-terminal fragment, with the site of attachment further localized by endoproteinase Lys-C cleavage to the region between Asn^{10} and Lys^{37}. The latter was shown to represent the first extracellular loop using further cleavage and sequencing of the wild-type and a mutant receptor. Following the same approach, the NO_2-Phe agonist probe was shown to also label the first extracellular loop region. Radiochemical sequencing identified that the Bpa antagonist probe labeled receptor residue Lys^{105}, whereas the NO_2-Phe agonist probe labeled residue Leu^{99}. These data extend our understanding of the molecular basis of binding and the conformational states of this important receptor.

Cholecystokinin (CCK) is a peptide hormone and neurotransmitter that plays important roles in nutrient homeostasis, regulating postcibal gallbladder contraction, pancreatic enzyme secretion, and gastrointestinal tract motility, while also being implicated in control of appetite. These functions support the broad potential of CCK receptors as drug targets. This goal of developing such drugs can be facilitated by a detailed understanding of the structure of the receptor mediating this action and by an understanding of the active and inactive conformations of this receptor.

CCK exhibits its agonist activities through binding to two subtypes of CCK receptors, types A and B, that represent structurally related members of the rhodopsin/β-adrenergic receptor family (class I) of G protein-coupled receptors (GPCRs) (Noble et al., 1999; Miller and Lybrand, 2002). The structural specificity of these receptors differ, with the type A receptor being most selective, requiring the carboxyl-terminal heptapeptide-amide of CCK with a sulfated tyrosyl residue, whereas the type B receptor requires only the carboxyl-terminal tetrapeptide for high-affinity binding and potent biological activity. In this work, we focus on the type A CCK receptor.

The molecular basis of ligand binding by the type A CCK receptor has been studied much more extensively than that of the type B CCK receptor, with studies using structure-activity (Bodanszky et al., 1977, 1980; Miller et al., 1981), mutagenesis (Kennedy et al., 1997; Gigoux et al., 1999; Gouldson et al., 2000; Ding et al., 2002), and photoaffinity labeling (Ji et al., 1997; Hadac et al., 1998, 1999; Ding et al., 2001; Arlander et al., 2004) approaches. These studies have suggested a theme analogous to that of many peptide receptors in the class I family of GPCRs (Schwartz, 1994; Strader et al., 1994), in which CCK binds to extracellular loop and amino-terminal tail regions of its receptor. Among all ap-

This work was supported by National Institutes of Health grant DK32878 and the Fiterman Foundation.
Article, publication date, and citation information can be found at http://molpharm.aspetjournals.org.
doi:10.1124/mol.105.012179.

ABBREVIATIONS: CCK, cholecystokinin; GPCR, G protein-coupled receptor; NO_2-Phe, *p*-nitro-phenylalanine; Bpa, *p*-benzoyl-L-phenylalanine; CNBr, cyanogen bromide; Lys-C, endoproteinase Lys-C; EF, endoglycosidase F; Bpa^{30} probe, des-amino-Tyr-Gly-[($Nle^{28,31}$,Bpa^{30})CCK-26-33]; NO_2-Phe^{30} probe, des-amino-Tyr-Gly-[($Nle^{28,31}$,NO_2-Phe^{30})CCK-26-33]; HPLC, high-performance liquid chromatography; CHO, Chinese hamster ovary; CCKR, cholecystokinin receptor; KRH, Krebs-Ringers-HEPES; MES, 2-(*N*-morpholino)ethanesulfonic acid.

proaches used, photoaffinity labeling is a method that provides direct specific residue-residue spatial approximations between a docked ligand and its receptor. We have previously used CCK agonist probes that incorporated photolabile residues within (in positions 27, 29, and 33) and outside (in position 24) the pharmacophore of the ligand (Ji et al., 1997; Hadac et al., 1998; Ding et al., 2001; Arlander et al., 2004) and demonstrated that they all labeled residues within the amino-terminal tail, and the second and third extracellular loop regions of this receptor. It should be noted that the first extracellular loop region has not been previously labeled by photolabile probes.

The tryptophan in position 30 of CCK is very interesting, located centrally within the pharmacophoric domain of the natural hormone. Spatial approximations between this ligand position and adjacent receptor residues have not previously been explored. Therefore, we have prepared a pair of CCK probes, one having a photolabile *p*-nitro-phenylalanine (NO_2-Phe) and another having a *p*-benzoyl-L-phenylalanine (Bpa) in this position. Here, we report their characterization and use in photoaffinity labeling studies to further explore their spatial approximations with the CCK receptor.

Materials and Methods

Materials. Synthetic CCK-8 (CCK-26-33) was purchased from Peninsula Laboratories (Belmont, CA). Wheat germ agglutinin-agarose was from E. Y. Labs (San Mateo, CA) and Fura-2 acetoxymethyl ester was from Molecular Probes (Eugene, OR). Cyanogen bromide (CNBr) and *m*-maleimidobenzoyl-*N*-hydroxysulfosuccinimide ester were from Pierce Chemical (Rockford, IL), and endoproteinase Lys-C was from Roche Diagnostics (Indianapolis, IN). *N*-(2-Aminoethyl-1)-3-aminopropyl glass beads were form Sigma-Aldrich (St. Louis, MO). Endoglycosidase F (EF) was prepared in our laboratory as reported previously (Pearson et al., 1987). All other reagents were analytical grade.

Peptides. The photolabile CCK analogs used in this study were des-amino-Tyr-Gly-[($Nle^{28,31}$,Bpa^{30})CCK-26-33] (Bpa^{30} probe) and des-amino-Tyr-Gly-[($Nle^{28,31}$,NO_2-Phe^{30})CCK-26-33] (NO_2-Phe^{30} probe) (Fig. 1). The former incorporated a photolabile Bpa moiety in position 30 to replace the native residue Trp, whereas the latter incorporated a photolabile NO_2-Phe in the same position. Each peptide also had an amino-terminal extension of Tyr-Gly to provide a site for radioiodination, and Met residues at position 28 and 31 were replaced with oxidation-resistant norleucine (Nle) residues. Each probe had its amino terminus blocked to permit radiochemical sequencing of the labeled receptor fragments without concomitant probe cleavage during cycles of Edman degradation. These modifications were well tolerated as we demonstrated previously (Ji et al., 1997; Hadac et al., 1998; Ding et al., 2001). These probes, together with the radioligand D-Tyr-Gly-[($Nle^{28,31}$)CCK-26-33] that was used for receptor-binding assays (Fig. 1), were synthesized by solid-phase techniques and purified by reversed-phase high-performance liquid chromatography (HPLC) (Powers et al., 1988). Their identities were confirmed by mass spectrometry. They were radioiodinated oxidatively with $Na^{125}I$ upon exposure to the solid-phase oxidant *N*-chloro-benzenesulfonamide (IODO beads; Pierce, Rockford, IL), for 15 s and purified by reversed-phase HPLC to yield specific radioactivities of 2000 Ci/mmol (Powers et al., 1988).

Receptor Sources. The receptor-bearing Chinese hamster ovary (CHO) cell line that was previously established to stably express the rat type A CCK receptor (CHO-CCKR) (Hadac et al., 1996) was used as the source of wild-type receptor in the current study. Another CHO cell line stably expressing the L104M mutant CCK receptor that was prepared and fully characterized previously (Arlander et al., 2004) was used for mapping the sites of labeling in this study. Cells were grown on tissue culture plasticware in Ham's F-12 medium supplemented with 5% fetal clone 2 (Hyclone Laboratories, Logan, UT) in a humidified atmosphere with 5% CO_2 at 37°C. Cells were passaged approximately twice a week and lifted mechanically before use. Plasma membranes were prepared from receptor-expressing cells using methods reported previously (Hadac et al., 1996), homogenized in Krebs-Ringers-HEPES (KRH) medium containing 25 mM HEPES, pH 7.4, 104 mM NaCl, 5 mM KCl, 2 mM $CaCl_2$, 1.2 mM $MgSO_4$, 1 mM KH_2PO_4, 0.01% soybean trypsin inhibitor, and 1 mM phenylmethylsulfonyl fluoride and stored at −80°C until ready for use.

Biological Activity Assay. The biological activity of the photolabile probes was studied using a well characterized assay for stimulation of intracellular calcium accumulation in CHO-CCKR cells (Hadac et al., 1996). In brief, approximately 2×10^6 cells were loaded with 5 μM Fura-2 acetoxymethyl ester in Ham's F-12 medium for 30 min at 37°C before being washed and stimulated with increasing concentrations of either the Bpa^{30} or NO_2-Phe^{30} probe or CCK at

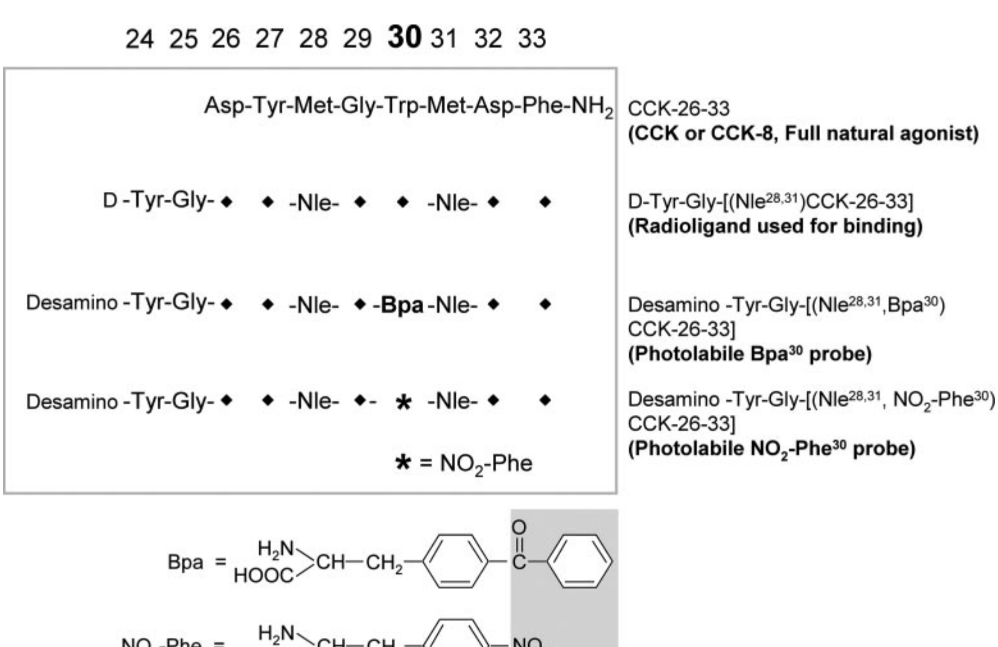

Fig. 1. Primary structures of CCK analogs used in this study. The Bpa^{30} and NO_2-Phe^{30} probes contained photolabile Bpa and NO_2-Phe residues in position 30. Shown also are the chemical structures of Bpa and NO_2-Phe, with their structural differences shaded in gray.

37°C. Fluorescence was quantified in a PerkinElmer Life and Analytical Sciences LS50B luminescence spectrometer. Excitation was performed at 340 and 380 nm, and emission was quantified at 520 nm, with calcium concentration calculated from the ratios, as described by Grynkiewicz et al. (1985). The peak intracellular calcium transient was used to determine agonist concentration dependence of the biological responses. Basal levels of calcium were measured in the absence of agonist stimulation, whereas maximum levels were determined as the peak intracellular calcium concentrations measured in the presence of a 1 μM CCK. Stimulated values were calculated as percentages of the range of calcium concentrations between basal and maximal levels. Treatment of cells with the Bpa^{30} probe alone elicited no calcium response. The antagonist activity of this probe was examined by its inhibition of the CCK-induced calcium response that was demonstrated by treating CHO-CCKR cells in the presence of 0.1 nM CCK in the presence of varied concentrations of the Bpa^{30} probe.

Binding Assay. The binding activity of the photoaffinity labeling probes was studied using a standard radioligand competition-binding assay using CHO-CCKR membranes, as we described previously (Hadac et al., 1996). In brief, 5 μg of plasma membranes were incubated with increasing concentrations (0–1 μM) of either the Bpa^{30} or NO_2-Phe^{30} probe or CCK in the presence of a constant amount of the radioiodinated radioligand D-Tyr-Gly-[($Nle^{28,31}$)CCK-26-33] (5 pM), for 1 h at room temperature in KRH medium containing 0.2% bovine serum albumin. Bound and free radioligand were separated using a Skatron cell harvester (Molecular Devices, Sunnyvale, CA) with glass fiber filtermats, with bound radioactivity quantified in a gamma counter. Nonspecific binding was determined in the presence of 1 μM CCK and represented less than 20% of total binding.

Photoaffinity Labeling. This was done using an established procedure that we described previously (Ding et al., 2001). In brief, 50 μg of plasma membranes from receptor-bearing CHO cells expressing wild-type or mutant receptors or from control non–receptor-bearing parental CHO cells was incubated with 0.1 nM radioiodinated Bpa^{30} or NO_2-Phe^{30} probe in the absence or presence of increasing concentrations of competing nonradioactive CCK (0–1 μM) for 1 h at room temperature in the dark. After incubation, the reactions were transferred to a ice-cold siliconized glass tubes (12 × 75 mm) for photolysis. This was performed for 30 min at 4°C in a Rayonet photochemical reactor (Southern New England Ultraviolet, Hamden, CT) equipped with 3500-Å (for the Bpa^{30} probe) or 3000-Å (for the NO_2-Phe^{30} probe) lamps. Membranes were then solubilized with 1% Nonidet P-40 in KRH medium before wheat-germ agglutinin-agarose affinity chromatography and subsequent SDS-polyacrylamide gel electrophoresis (Laemmli, 1970). Radiolabeled bands were visualized by autoradiography.

Peptide Mapping. To map the regions of receptor labeling using chemical cleavage and subsequent sequencing, it was necessary to prepare affinity-labeled receptor in larger scale. For this, 200 μg of receptor-bearing membranes and 0.5 nM ^{125}I-Bpa^{30} or ^{125}I-NO_2-Phe^{30} probe were incubated in the absence of competing CCK before photolysis. After electrophoresis, radioactive protein bands were excised from polyacrylamide gels, eluted with water, lyophilized, ethanol-precipitated, and cleaved with 2.5 mg of CNBr in 70% formic acid, as described in detail previously (Hadac et al., 1998). Samples were then washed twice with water and dried in a vacuum centrifuge before being resolved on a 10% NuPAGE gel using MES running buffer (Invitrogen, Carlsbad, CA). Deglycosylation was performed on gel-purified receptor or fragment using conditions described previously (Hadac et al., 1996), and the products were analyzed on 10% SDS-polyacrylamide gels (for intact receptor) or 10% NuPAGE gels (for receptor fragments), and labeled bands were visualized by autoradiography.

Identification of the domain of labeling of the CCK receptor by the Bpa^{30} probe was also achieved by Edman degradation sequencing of the purified CNBr fragments of the labeled receptor using strategies described previously (Hadac et al., 1998; Dong et al., 2004). In brief, 10 mg of CHO-CCKR plasma membranes photoaffinity labeled with 0.1 μM nonradioactive Bpa^{30} probe were mixed with 1 mg of membranes labeled with 1 nM ^{125}I-Bpa^{30} probe and were gel-purified by the procedure described above. The labeled receptor was further cleaved by CNBr, and the resultant fragments were purified by the procedure described that included 10% NuPAGE gel electrophoresis and microbore C18 HPLC before being subjected to Edman degradation sequencing using an Applied Biosystems automated instrument (Hadac et al., 1998; Dong et al., 2004).

Radiochemical Sequencing. Gel-purified CNBr fragments from cleavage of labeled wild type and L104M mutant CCK receptor constructs were used for radiochemical Edman degradation sequencing to localize the receptor residues labeled by both the Bpa^{30} and NO_2-Phe^{30} probes. Sequencing was performed on cysteine-containing CNBr fragments (Pro^{96}-Met^{121} from the wild-type receptor and Lys^{105}-Met^{121} from the L104M mutant receptor) of the receptor that were immobilized through the thiol group of Cys^{114} using the bifunctional cross-linker *m*-maleimidobenzoyl-*N*-hydroxysulfosuccinimide ester and *N*-(2-aminoethyl-1)-3-aminopropyl glass beads. Edman degradation was manually repeated in a manner that has been reported previously in detail (Ji et al., 1997; Hadac et al., 1998), and the radioactivity released in each cycle was quantified in a gamma spectrometer.

Statistical Analysis. All observations were repeated at least three times in independent experiments and are expressed as mean ± S.E.M. Binding data were analyzed and plotted using the nonlinear regression analysis routine for radioligand binding in the Prism software package (GraphPad Software Inc., San Diego, CA), and binding kinetics was determined by analysis with the LIGAND program of Munson and Rodbard (1980).

Results

Probe Characterization. The photoaffinty labeling probes used in this study were des-amino-Tyr-Gly-[($Nle^{28,31}$,Bpa^{30})CCK-26-33] (Bpa^{30} probe) and des-amino-Tyr-Gly-[($Nle^{28,31}$,NO_2-Phe^{30})CCK-26-33] (NO_2-Phe^{30} probe) (Fig. 1). Both incorporated a photolabile residue at position 30 to replace the naturally occurring Trp residue, with one probe having a Bpa and the other having a NO_2-Phe. Both probes were synthesized by solid-phase techniques and purified by reversed-phase HPLC. They were characterized to demonstrate the expected molecular masses by matrix-assisted laser desorption/ionization-time of flight mass spectrometry.

Probe usefulness in photoaffinity labeling studies was first evaluated by characterization of binding and biological activity. As shown in Fig. 2, both probes bound to the CCK receptor specifically and saturably, although with lower affinity than natural CCK (K_i values: CCK, 0.9 ± 0.1 nM; Bpa^{30} probe, 270 ± 72 nM; and NO_2-Phe^{30} probe, 180 ± 40 nM). Although less potent than natural CCK, the NO_2-Phe^{30} probe was a full agonist, stimulating intracellular calcium accumulation in CHO-CCKR cells in a concentration-dependent manner (EC_{50} values: CCK, 9.2 ± 2.3 pM; and NO_2-Phe^{30} probe, 81 ± 15 nM). However, the Bpa^{30} probe was an antagonist, having no endogenous agonist activity at a concentration as high as 1 μM (Fig. 2). It inhibited 0.1 nM CCK-stimulated calcium signaling in a concentration-dependent manner (IC_{50} = 2.0 ± 0.1 μM, Fig. 2). Thus, we have developed a pair of structurally related photoaffinity labeling probes having their photolabile site of covalent attachment in the same position within the pharmacophore of CCK, but having distinct biological activities, one representing a full agonist and the other an antagonist.

Photoaffinity Labeling of the CCK Receptor. Both the Bpa^{30} and NO_2-Phe^{30} probes were used to examine their ability to label the CCK receptor. Figure 3 shows that both probes covalently labeled the CCK receptor specifically and saturably, with the labeling inhibited by natural CCK in a concentration-dependent manner (IC_{50} values: Bpa^{30} probe, 15.5 ± 2.9 nM; and NO_2-Phe^{30} probe, 36 ± 4 nM). Consistent with previous photoaffinity labeling studies of this receptor (Ji et al., 1997; Hadac et al., 1998; Ding et al., 2001; Arlander et al., 2004), the band labeled by each probe migrated at approximate M_r = 85,000 to 95,000 and shifted to approximate M_r = 42,000 after deglycosylation with endoglycosidase F. Attempts to label non–receptor-bearing CHO cell membranes did not yield visible radioactive bands on the gel.

Mapping the Receptor Ligand-Binding Domain. The receptor regions covalently labeled by the probes were examined using proteolytic cleavage. CNBr was used to provide the first indication because of its high efficiency of cleavage. The CCK receptor contains 15 Met residues, representing the sites of CNBr cleavage, theoretically resulting in 16 fragments with molecular masses ranging from 0.1 to 9.9 kDa, with two fragments containing potential sites for *N*-glycosylation (Fig. 4). Figure 4 shows the CNBr cleavage patterns for CCK receptor labeled by each of the probes. As shown, the Bpa^{30} probe labeled two fragments, a glycosylated fragment migrating at approximate M_r = 25,000 and shifting to approximate M_r = 8500 after deglycosylation, and a nonglycosylated fragment migrating at approximate M_r = 4500. Considering the mass of the attached probe (1378 Da) and the nature of glycosylation, the glycosylated fragment represented the segment Asn^{10}-Met^{72} that contained the amino terminus and the first transmembrane domain of the recep-

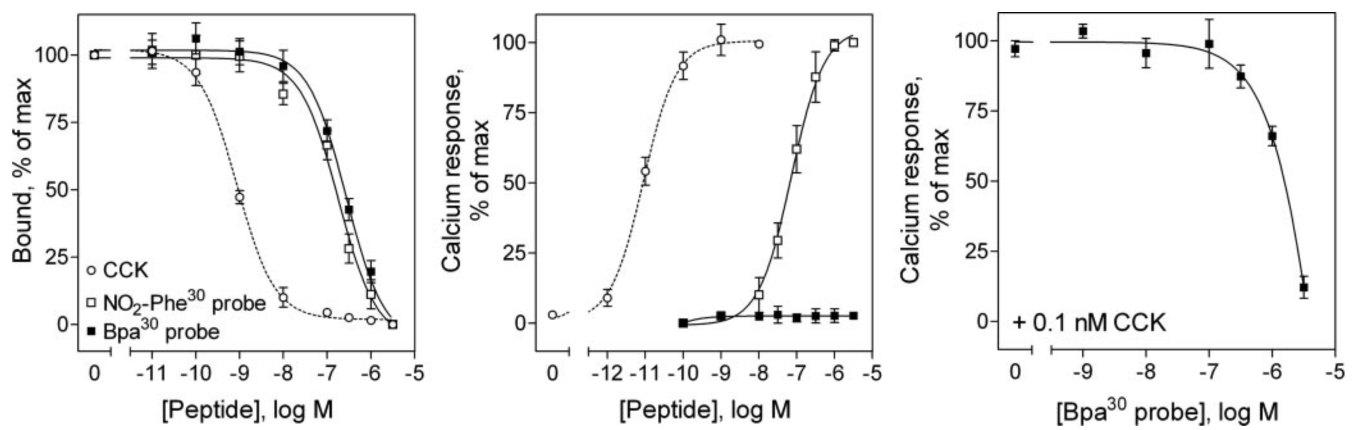

Fig. 2. Functional characterization of the photoaffinity labeling probes. Left, abilities of increasing concentrations of indicated CCK analogs to compete for binding of the radioligand ^{125}I-D-Tyr-Gly-[(Nle^{28,31})CCK-26-33], to membranes from CHO-CCKR cells. Values are calculated as percentages of maximal saturable binding observed in the absence of competitor. They are expressed as means ± S.E.M. of duplicate data from three independent experiments. Middle, ability of increasing concentrations of indicated CCK analogs to stimulate intracellular calcium responses in CHO-CCKR cells. The basal level of intracellular calcium concentration was 137 ± 28 nM, with the stimulated levels reaching a maximum of 325 ± 44 nM. Right, ability of the Bpa^{30} probe to inhibit a CCK-stimulated intracellular calcium response. Values are expressed as means ± S.E.M. of data from a minimum of three independent experiments.

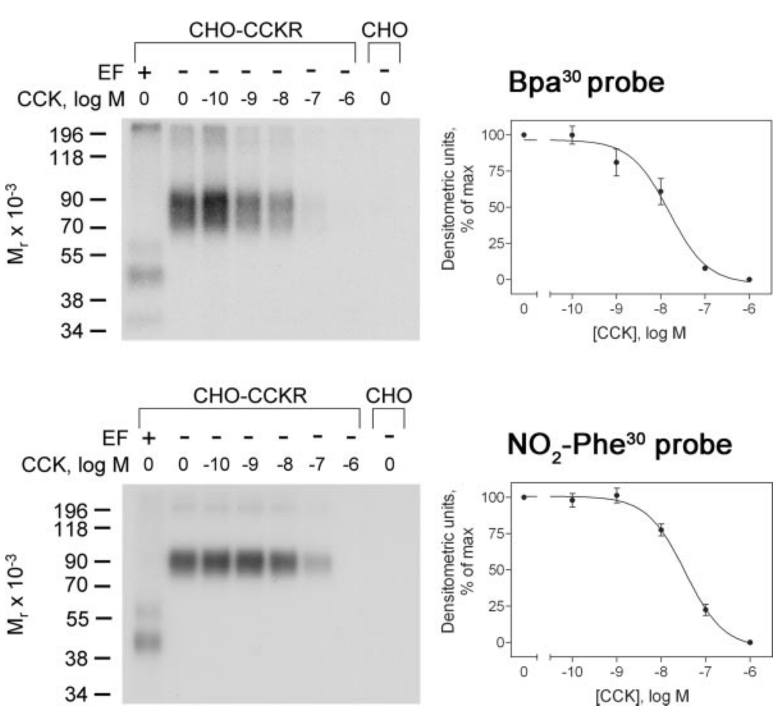

Fig. 3. Photoaffinity labeling of the CCK receptor. Shown are typical autoradiographs of 10% SDS-polyacrylamide electrophoresis gels used to separate products of affinity labeling with the Bpa^{30} (top) or NO_2-Phe^{30} (bottom) probes. CHO-CCKR membranes were labeled by each probe in the absence or presence of increasing concentrations of competing unlabeled CCK. Nonreceptor bearing CHO membranes labeled by each probe are also shown. The affinity-labeled rat CCK receptor migrated at approximate M_r = 85,000 to 95,000 and shifted to M_r = 42,000 after deglycosylation with EF. Right, densitometric analyses of the receptor labeling in the presence of increasing concentrations of competing CCK in three independent experiments (means ± S.E.M.).

MOL PHARM
MOLECULAR PHARMACOLOGY

tor (see below for further identification). The candidates for the nonglycosylated fragment included all three extracellular loop fragments because of their similar masses.

Distinct from labeling by the Bpa^{30} probe, the NO$_2$-Phe^{30} probe only labeled a nonglycosylated receptor fragment migrating at approximate M_r = 4500. Considering the molecular mass of the attached probe (1357 Da), the expected fragment would be in the range of ~2 to 3 kDa, and candidates also included fragments within all the extracellular loop domains.

The CNBr fragment from the CCK receptor labeled by the Bpa^{30}-probe was extensively purified to chemical homogeneity as described under *Materials and Methods* and was subjected to Edman degradation sequencing. This resulted in the identification of the sequence Pro-Phe-Asn-Leu-Ile-Pro-Asn-Leu-Leu in cycles 1 to 9. This sequence exists only in the rat type A CCK receptor and corresponds with the first nine residues of the CNBr fragment spanning the first extracellular loop (Pro^{96}-Met^{121}). This provided definitive identification of the fragment Pro^{96}-Met^{121} as one of the two regions labeled by the Bpa^{30} probe. This was further confirmed by CNBr cleavage of the L104M CCK receptor mutant (Arlander et al., 2004) labeled by the Bpa^{30} probe, which resulted in a small but significant shift of the approximate M_r = 4500 fragment in the labeled wild-type receptor to approximate M_r = 4000 in the L104M mutant (Fig. 5).

Likewise, the L104M receptor construct was also used to test whether the NO$_2$-Phe^{30} probe labeled this CNBr fragment. As shown in Fig. 5, CNBr cleavage of the L104M receptor mutant labeled with the NO$_2$-Phe^{30} probe yielded a significant shift to approximate M_r = 3000 from the approximate M_r = 4500 fragment in the labeled wild-type receptor. This confirmed that the NO$_2$-Phe^{30} agonist probe labeled the CNBr fragment Pro^{96}-Met^{121} that included the first extracellular loop, the same fragment as that labeled by the Bpa^{30} antagonist probe, although likely at a different site.

Of note, the Bpa^{30} probe also labeled the glycosylated fragment Asn^{10}-Met^{72} as described above. Further localization was achieved with subsequent endoproteinase Lys-C treatment. As shown in Fig. 6, cleavage of the labeled M_r = 25,000 CNBr fragment with this protease yielded a band migrating at approximate M_r = 22,000 that further shifted to approximate M_r = 4500 after deglycosylation. This further refined the region of labeling with the Bpa^{30} probe as between Asn^{10} and Lys^{37} within the extracellular amino terminus of the CCK receptor.

Identification of Distinct Sites of Labeling by the Bpa^{30} Antagonist and NO$_2$-Phe^{30} Agonist Probes. Radiochemical sequencing was used to identify the specific receptor residues labeled by each probe. For this, CNBr fragments from both the wild type (Pro^{96}-Met^{121}) and L104M mutant (Lys^{105}-Met^{121}) receptors labeled by each probe were purified to radiochemical homogeneity and coupled to *N*-(2-aminoethyl-1)-3-aminopropyl glass beads through Cys^{114} for manual Edman degradation sequencing. As shown in Fig. 7, a radioactive peak eluted in cycle 1 when sequencing the Lys^{105}-Met^{121} fragment from the L104M mutant labeled by the Bpa^{30} antagonist probe, whereas no peak was found when sequencing the Pro^{96}-Met^{121} fragment from the wild-type receptor labeled with the same probe. This indicated that the probe specifically labeled the residue Lys^{105} of the receptor. Shown also in Fig. 7 is the radioactivity elution profile of sequencing the radiochemically pure CNBr fragments labeled by the NO$_2$-Phe^{30} probe. A peak eluted in cycle

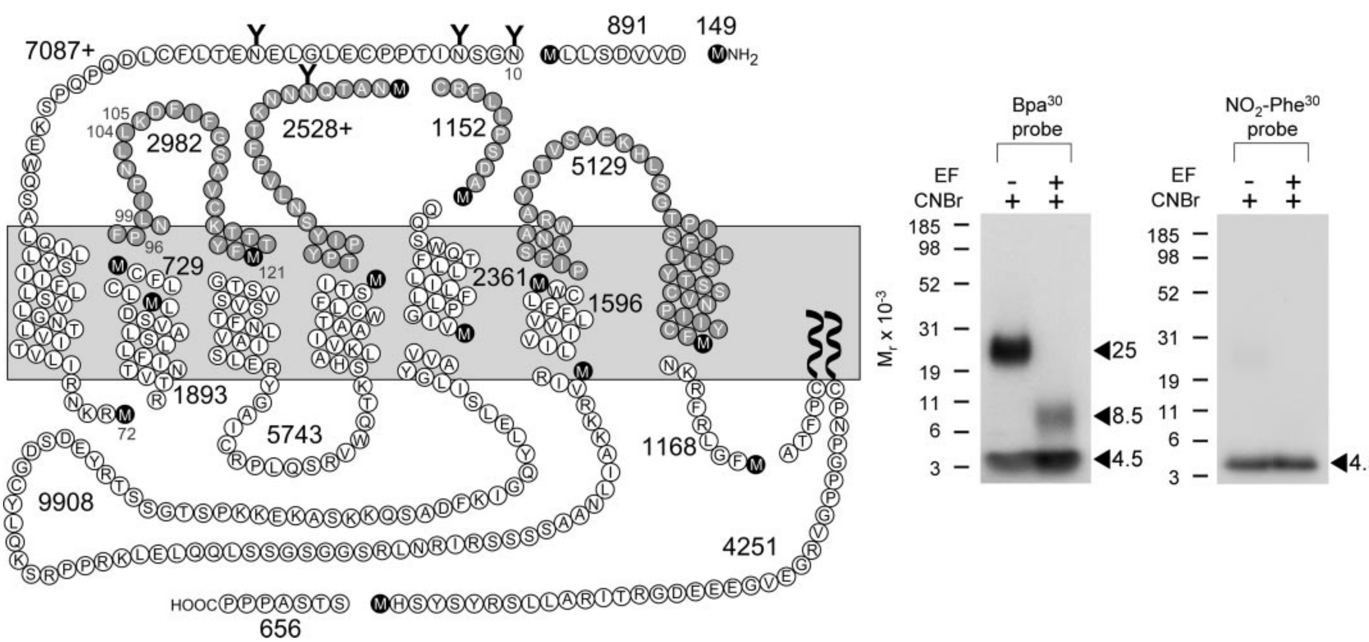

Fig. 4. Mapping labeled domains by CNBr cleavage. Left, diagram illustrating the theoretical sites of CNBr cleavage within the CCK receptor, with the masses of the predicted fragments. Middle and right, representative autoradiographs of 10% Nu-PAGE gels used to separate the products of CNBr cleavage of the native and deglycosylated CCK receptor that had been labeled with the Bpa^{30} (middle) and NO$_2$-Phe^{30} (right) probe. CNBr cleavage of the receptor labeled by the Bpa^{30} probe yielded a glycosylated fragment migrating at approximate M_r = 25,000 that shifted to approximate M_r = 8500 after deglycosylation by EF, and a nonglycosylated fragment migrating at M_r = 4500. The former represents the glycosylated receptor fragment Asn^{10}-Met^{72} at the amino terminus. The candidates for the latter included all extracellular loop fragments. The cleavage of the receptor labeled by the NO$_2$-Phe^{30} (right) probe resulted in a single nonglycosylated fragment migrating at approximate M_r = 4500. The candidates for this fragment also included all extracellular loop fragments. These data are representative of at least three independent experiments.

MOL PHARM

4 when sequencing the Pro^{96}-Met^{121} fragment from the wild-type receptor labeled by the NO_2-Phe^{30} probe, whereas no peak was found when sequencing the Lys^{105}-Met^{121} fragment from the L104M mutant labeled with the same probe. This identified the receptor residue Leu^{99} as the site of labeling by the NO_2-Phe^{30} agonist probe.

Discussion

Understanding the molecular basis of ligand binding to physiologically important receptors and the conformational changes associated with activation of these receptors is critical for rational structure-based drug design. GPCRs repre-

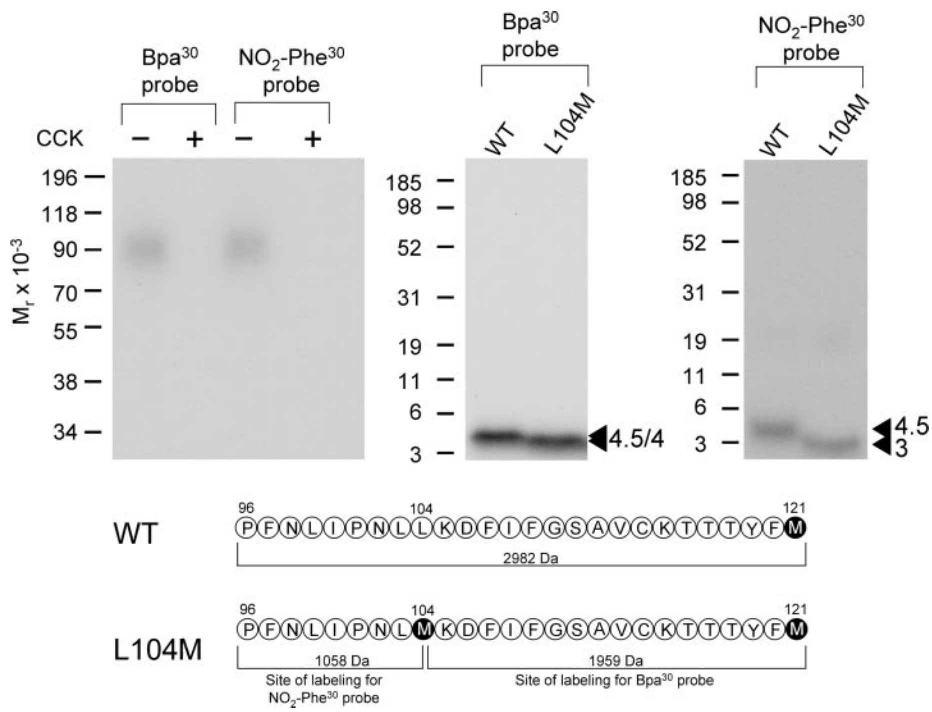

Fig. 5. Photoaffinity labeling and CNBr cleavage of the L104M CCK receptor mutant. Left, L104M CCK receptor mutant was labeled specifically and efficiently by both probes. Middle and right, representative autoradiographs of the CNBr cleavage of the wild-type (WT) and L104M CCK mutant receptors labeled by the Bpa^{30} (middle) and NO_2-Phe^{30} (right) probe. CNBr cleavage of the L104M CCK receptor mutant labeled by the Bpa^{30} probe yielded a labeled band migrating at approximate $M_r = 4000$, distinctly from the $M_r = 4500$ CNBr fragment from the labeled WT receptor, indicating the fragment (Pro^{96}-Met^{121}) spanning the first extracellular loop contained the site of labeling for the Bpa^{30} probe. Considering the mass of the attached probe (1378 Da), the Lys^{105}-Met^{121} segment was felt most likely to contain the site of labeling for the Bpa^{30} probe (bottom). CNBr cleavage of the L104M CCK mutant receptor labeled by the NO_2-Phe^{30} probe yielded a similar cleavage pattern, with the labeled band migrating at approximate $M_r = 3000$, indicating this probe labeled the same fragment as the Bpa^{30} probe but probably within a different segment. Considering the mass of the attached probe (1357 Da), the site of labeling for the NO_2-Phe^{30} probe was felt to be most likely within the region Pro^{96}-Met^{104} (bottom). These data are representative of three independent experiments.

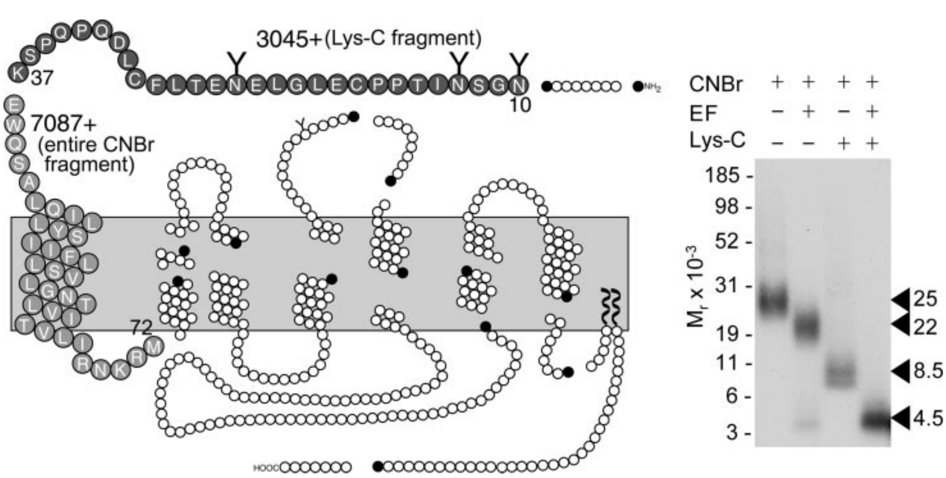

Fig. 6. Identification of the second site of CCK receptor labeled with the agonist probe. Left, a diagram of the theoretical sites of cleavage of the CCK receptor, highlighting the CNBr fragment of interest. Right, a typical autoradiograph of a 10% NuPAGE gel used to separate the products of sequential endoproteinase Lys-C cleavage of the purified $M_r = 25{,}000$ CNBr fragment representing receptor fragment Asn^{10}-Met^{72} labeled with the Bpa^{30} agonist probe. As shown, further Lys-C cleavage of this fragment yielded a band migrating at approximate $M_r = 22{,}000$ that shifted to apparent $M_r = 4500$ after deglycosylation by EF. This further localized the site of labeling to the region between Asn^{10} and Lys^{37}, as highlighted in dark gray in the diagram on the left. These data are representative of three independent experiments.

MOLECULAR PHARMACOLOGY

sent the largest group of receptors in the body that includes many important drug targets. Although high-resolution biophysical techniques such as NMR or X-ray crystallography are the preferred methods for gaining insights into the detailed structural features of receptor-ligand complexes, these have been difficult to apply to this group of molecules, because of their natural sparsity, extreme hydrophobicity, and difficulty in purification and crystallization. The only extant high-resolution three-dimensional crystal structure of an intact member of this superfamily is that of rhodopsin in its inactive state (Palczewski et al., 2000).

The CCK receptor represents a potentially important drug target, having diverse physiological actions at multiple targets along the gastrointestinal tract and brain. Because it is structurally related to rhodopsin, belonging to the class I family of GPCRs, the confluence of transmembrane helices probably resembles that structure. However, the extracellular loop and tail domains of the CCK receptor that have been implicated as playing important roles in natural peptide ligand recognition are probably very different from rhodopsin (Ding et al., 2002). Current insight into these regions of the CCK receptor is based largely on the indirect observations provided by receptor mutagenesis and by ligand structure-activity relationships (Bodanszky et al., 1977, 1980; Miller et al., 1981; Kennedy et al., 1997; Gigoux et al., 1999; Gouldson et al., 2000; Ding et al., 2002) and on direct observations of residue-residue approximations determined using photoaffinity labeling studies with docked photolabile ligand probes (Ji et al., 1997; Hadac et al., 1998; Hadac et al., 1999; Ding et al., 2001; Arlander et al., 2004).

Photoaffinity labeling is a powerful tool to establish spatial approximations between specific residues within a ligand and within its receptor as complexed together. Using this approach, we have previously established such constraints for residues at the carboxyl terminus (position 33), midregion (positions 29), and extension of the amino terminus (position 24) of the pharmacophores of full agonist CCK analogs. The position 33 probe labels Trp^{39} within the amino terminus of the CCK receptor (Ji et al., 1997), whereas position 29 probe labels His^{347} and Leu^{348} within the third extracellular loop (Hadac et al., 1998), and the position 24 probe labels a dominant site within the third loop (Glu^{345}) as well as a minor site in the amino terminus of the receptor, between Asn^{10} and Lys^{37} (Ding et al., 2001).

These constraints have been used to build and subsequently refine molecular models of the CCK agonist-bound receptor (Ding et al., 2001). These have resulted in a model in which the carboxyl terminus of CCK is sited near receptor amino terminal residue Trp^{39} just above the first transmembrane segment and the amino terminus of the natural peptide ligand is oriented away from the lipid bilayer (Dawson et al., 2002). This is in distinct contrast with another model proposed by the Fourmy group that is based on receptor mutagenesis data, in which the peptide is docked with its carboxyl terminus situated within the confluence of transmembrane helices adjacent to transmembrane segment six (Escrieut et al., 2002). Our proposed model for the active complex of agonist docked to this receptor has recently been further validated by fluorescence resonance energy transfer analysis, with distances from CCK determined to each of the extracellular loop regions (Harikumar and Miller, 2002). No models have yet been proposed for the peptide antagonist-bound CCK receptor in its inactive state.

We recently provided the first insights into the changes in conformation associated with active and inactive states of the CCK receptor using photolabile position 27 agonist and antagonist probes (Arlander et al., 2004). In that work, direct photoaffinity labeling with a full agonist probe confirmed the spatial approximation of this residue with receptor residue Arg^{197} within the second loop in the active complex. However, the analogous photolabile position 27 antagonist probe was shown to label a distinct region within the receptor amino terminus. These data demonstrated a key structural difference in active and inactive complexes of the ligand-bound CCK receptor.

The current work continues our efforts to obtain additional constraints for refining our agonist-bound CCK receptor model and provides additional insights into the differences in molecular approximation between active and inactive states of the CCK receptor by using structurally related antagonist probes. We now focus on the tryptophan in position 30 of CCK. Although this residue has been shown to be important for full agonist activity at the type A CCK receptor, it can be substituted by norleucine (Rolland et al., 1991) or 6-NO_2-Trp (Klueppelberg et al., 1989) without loss of affinity or potency. Although the latter peptide (^{125}I-D-Tyr-Gly-[($Nle^{28,31}$,6-NO_2-Trp^{30})CCK-26-33]) was able to covalently label the receptor, the efficiency of covalent attachment was not adequate to identify adjacent residues.

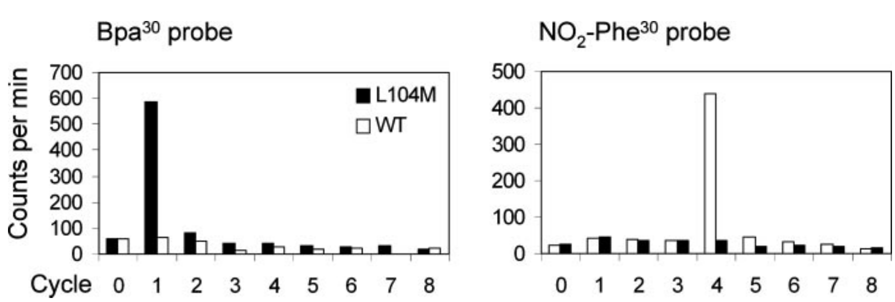

Fig. 7. Identification of the labeled receptor residues. Left, representative radioactivity elution profiles from sequencing of the CNBr fragments from the wild-type (WT) and L104M mutant CCK receptors labeled with the Bpa^{30} antagonist probe. A peak in radioactivity occurred in elution cycle 1 for the L104M mutant receptor, representing the labeled receptor residue Lys^{105}. No peak was observed in the profile of sequencing the CNBr fragment from the wild-type CCK receptor labeled by the same probe. Right, representative radioactivity elution profiles from sequencing of the CNBr fragments from the wild type and L104M mutant CCK receptors labeled with the NO_2-Phe^{30} probe. There was a peak in radioactivity eluted in cycle 4 for the wild-type receptor that corresponds with covalent labeling of residue Leu^{99} of the receptor. No peak was observed in the profile of sequencing the CNBr fragment from the L104M mutant CCK receptor labeled by the same probe. These data are representative of three independent experiments.

In the current work, Trp[30] was replaced by a photolabile NO_2-Phe moiety, and the resultant probe retained full efficacy of biological activity and also yielded high-efficiency covalent attachment to permit such identification. In another analog of this peptide, Trp[30] was replaced by a photolabile Bpa moiety, resulting in an antagonist, rather than an agonist. Because the Bpa moiety is larger than either the 6-NO_2-Trp or NO_2-Phe moieties, which are closer in size to the natural Trp present in that position, it is possible that steric hindrance was responsible for the inability of the Bpa analog to achieve an active conformation. It is unclear whether a constrained peptide conformation or interference with the peptide-receptor interaction was responsible, but the net effect was to yield binding affinity similar to the analogous agonist probe, but no intrinsic biological activity. Thus, we have developed a pair of analogous agonist and antagonist photolabile probes, with the only structural difference being the photolabile residue in position 30.

It is of note that the NO_2-Phe[30] agonist probe in this study labeled CCK receptor residue Leu[99] within the predicted first extracellular loop. This is a region that includes residues with substantial impact in mutagenesis studies of both the type A (Silvente-Poirot et al., 1998; Gouldson et al., 2000) and type B (Silvente-Poirot et al., 1998) CCK receptors. This region is clearly distinct from type A CCK receptor regions previously demonstrated to be adjacent to the carboxyl terminus (position 33), mid-region (position 27 and 29), and the amino-terminal extension (position 24) of the pharmacophore of CCK (Ji et al., 1997; Hadac et al., 1998; Ding et al., 2001; Arlander et al., 2004). However, it is consistent with analogous labeling of the type B CCK receptor using the same position 33 and 24 probes (Dong et al., 2005). This spatial approximation is fully compatible with the model we recently proposed for the peptide agonist ligand-occupied CCK receptor (Ding et al., 2001).

It is also notable that one of the regions of labeling by the Bpa[30] antagonist probe was similar to that for the NO_2-Phe[30] agonist probe. This supports the general similarity in docking the structurally related agonist and antagonist probes, as we previously observed for structurally related agonist, partial agonist, and antagonist probes that had a photolabile Bpa situated at their amino terminus (Dong et al., 1999). Although both the agonist and antagonist used in the current study labeled the same receptor region, the specific residues that were labeled were distinct, with the Bpa[30] antagonist probe labeling Lys[105] and the NO_2-Phe[30] agonist probe labeling Leu[99]. Mutagenesis of Lys[105] has previously been shown to be well tolerated for agonist action, consistent with absence of direct functional importance (Gouldson et al., 2000).

The Bpa[30] antagonist probe also labeled a second receptor region, the receptor amino terminus between Asn[10] and Lys[37]. This region can be truncated without significant negative impact on receptor ligand binding or agonist-stimulated signaling (Kennedy et al., 1995; Ding et al., 2001). This was also the region labeled by position 33 and position 24 agonist probes (Ji et al., 1997; Ding et al., 2001), as well as by the position 27 antagonist probe (Arlander et al., 2004). These data are consistent with the amino terminus covering the peptide-binding domain of this receptor, but not playing a significant direct functional role, as was proposed previously (Ding et al., 2001).

In summary, we have now prepared a pair of structurally-related CCK agonist and antagonist probes that each incorporated a photolabile residue into position 30 of the ligand and have used them to explore the residue-residue approximations as docked at the CCK receptor in active and inactive states. Both labeled the same region of the CCK receptor (the first extracellular loop) that is distinct from regions labeled previously by probes of this receptor, providing further important confirmation of the evolving molecular model. The distinct sites of labeling within this region provide additional insights into the differences between active and inactive conformations of this receptor.

Acknowledgments

We thank Eileen L. Holicky for excellent technical assistance, Dana Huether for secretarial assistance, and Benjamin J. Madden (Mayo Clinic Protein Core Facility) for helping with protein sequencing.

References

Arlander SJ, Dong M, Ding XQ, Pinon DI, and Miller LJ (2004) Key differences in molecular complexes of the cholecystokinin receptor with structurally related peptide agonist, partial agonist and antagonist. *Mol Pharmacol* **66:**545–552.

Bodanszky M, Natarajan S, Hahne W, and Gardner JD (1977) Cholecystokinin (pancreozymin). 3. Synthesis and properties of an analogue of the C-terminal heptapeptide with serine sulfate replacing tyrosine sulfate. *J Med Chem* **20:**1047–1050.

Bodanszky M, Tolle JC, Gardner JD, Walker MD, and Mutt V (1980) Cholecystokinin (pancreozymin). Synthesis and properties of the N alpha-acetyl-derivative of cholecystokinin 27–33. *Int J Pept Protein Res* **16:**402–411.

Dawson ES, Henne RM, Miller LJ, and Lybrand TP (2002) Moleular models for cholecystokinin-A receptor. *Pharmacol Toxicol* **91:**290–296.

Ding XQ, Dolu V, Hadac EM, Holicky EL, Pinon DI, Lybrand TP, and Miller LJ (2001) Refinement of the structure of the ligand-occupied cholecystokinin receptor using a photolabile amino-terminal probe. *J Biol Chem* **276:**4236–4244.

Ding XQ, Pinon DI, Furse KE, Lybrand TP, and Miller LJ (2002) Refinement of the conformation of a critical region of charge-charge interaction between cholecystokinin and its receptor. *Mol Pharmacol* **61:**1041–1052.

Dong M, Ding XQ, Pinon DI, Hadac EM, Oda RP, Landers JP, and Miller LJ (1999) Structurally related peptide agonist, partial agonist and antagonist occupy a similar binding pocket within the cholecystokinin receptor. Rapid analysis using fluorescent photoaffinity labeling probes and capillary electrophoresis. *J Biol Chem* **274:**4778–4785.

Dong M, Li Z, Pinon DI, Lybrand TP, and Miller LJ (2004) Spatial approximation between the amino terminus of a peptide agonist and the top of the sixth transmembrane segment of the secretin receptor. *J Biol Chem* **279:**2894–2903.

Dong M, Liu G, Pinon, PI, and Miller LJ (2005) Differential docking of high-affinity peptide ligands to type A and B cholecystokinin receptors demonstrated by photoaffinity labeling. *Biochemistry*, in press.

Escrieut C, Gigoux V, Archer E, Verrier S, Maigret B, Behrendt R, Moroder L, Bignon E, Silvente-Poirot S, Pradayrol L, et al. (2002) The biologically crucial C terminus of cholecystokinin and the non-peptide agonist SR-146,131 share a common binding site in the human CCK1 receptor. Evidence for a crucial role of Met-121 in the activation process. *J Biol Chem* **277:**7546–7555.

Gigoux V, Maigret B, Escrieut C, Silvente-Poirot S, Bouisson M, Fehrentz JA, Moroder L, Gully D, Martinez J, Vaysse N, et al. (1999) Arginine 197 of the cholecystokinin-A receptor binding site interacts with the sulfate of the peptide agonist cholecystokinin. *Protein Sci* **8:**2347–2354.

Gouldson P, Legoux P, Carillon C, Dumont X, Le Fur G, Ferrara P, and Shire D (2000) Essential role of extracellular charged residues of the human CCK(1) receptor for interactions with SR 146131, SR 27897 and CCK-8S. *Eur J Pharmacol* **389:**115–124.

Grynkiewicz G, Poenie M, and Tsien RY (1985) A new generation of Ca^{2+} indicators with greatly improved fluorescence properties. *J Biol Chem* **260:**3440–3450.

Hadac EM, Ghanekar DV, Holicky EL, Pinon DI, Dougherty RW, and Miller LJ (1996) Relationship between native and recombinant cholecystokinin receptors: role of differential glycosylation. *Pancreas* **13:**130–139.

Hadac EM, Ji Z, Pinon DI, Henne RM, Lybrand TP, and Miller LJ (1999) A peptide agonist acts by occupation of a monomeric G protein-coupled receptor: dual sites of covalent attachment to domains near TM1 and TM7 of the same molecule make biologically significant domain-swapped dimerization unlikely. *J Med Chem* **42:**2105–2111.

Hadac EM, Pinon DI, Ji Z, Holicky EL, Henne RM, Lybrand TP, and Miller LJ (1998) Direct identification of a second distinct site of contact between cholecystokinin and its receptor. *J Biol Chem* **273:**12988–12993.

Harikumar KG and Miller LJ (2002) Applications of fluorescence in the characterization of the ligand-binding domain and activation of the cholecystokinin receptor. *Pharmacol Toxicol* **91:**286–289.

Ji Z, Hadac EM, Henne RM, Patel SA, Lybrand TP, and Miller LJ (1997) Direct identification of a distinct site of interaction between the carboxyl-terminal residue of cholecystokinin and the type A cholecystokinin receptor using photoaffinity labeling. *J Biol Chem* **272:**24393–243401.

Kennedy K, Escrieut C, Dufresne M, Clerc P, Vaysse N, and Fourmy D (1995) Identification of a region of the N-terminal of the human CCKA receptor essential for the high affinity interaction with agonist CCK. *Biochem Biophys Res Commun* **213:**845–852.
Kennedy K, Gigoux V, Escrieut C, Maigret B, Martinez J, Moroder L, Frehel D, Gully D, Vaysse N, and Fourmy D (1997) Identification of two amino acids of the human cholecystokinin-A receptor that interact with the N-terminal moiety of cholecystokinin. *J Biol Chem* **272:**2920–2926.
Klueppelberg UG, Gaisano HY, Powers SP, and Miller LJ (1989) Use of a nitrotryptophan-containing peptide for photoaffinity labeling the pancreatic cholecystokinin receptor. *Biochemistry* **28:**3463–3468.
Laemmli UK (1970) Cleavage of structural proteins during the assembly of the head of bacteriophage T4. *Nature (Lond)* **227:**680–685.
Miller LJ and Lybrand TP (2002) Molecular basis of agonist binding to the type A cholecystokinin receptor. *Pharmacol Toxicol* **91:**282–285.
Miller LJ, Rosenzweig SA, and Jamieson JD (1981) Preparation and characterization of a probe for the cholecystokinin octapeptide receptor, N α (^{125}I-desaminotyrosyl-)CCK-8 and its interactions with pancreatic acini. *J Biol Chem* **256:**12417–12423.
Munson PJ and Rodbard D (1980) Ligand: a versatile computerized approach for characterization of ligand-binding systems. *Anal Biochem* **107:**220–239.
Noble F, Wank SA, Crawley JN, Bradwejn J, Seroogy KB, Hamon M, and Roques BP (1999) International Union of Pharmacology. XXI. Structure, distribution and functions of cholecystokinin receptors. *Pharmacol Rev* **51:**745–781.
Palczewski K, Kumasaka T, Hori T, Behnke CA, Motoshima H, Fox BA, Le Trong I, Teller DC, Okada T, Stenkamp RE, et al. (2000) Crystal structure of rhodopsin: a G protein-coupled receptor. *Science (Wash DC)* **289:**739–745.
Pearson RK, Miller LJ, Hadac EM, and Powers SP (1987) Analysis of the carbohydrate composition of the pancreatic plasmalemmal glycoprotein affinity labeled by short probes for the cholecystokinin receptor. *J Biol Chem* **262:**13850–13856.
Powers SP, Pinon DI, and Miller LJ (1988) Use of *N*,*O*-bis-Fmoc-D-Tyr-ONSu for introduction of an oxidative iodination site into cholecystokinin family peptides. *Int J Pept Protein Res* **31:**429–434.
Rolland M, Rodriguez M, Lignon MF, Galas MC, Laur J, Aumelas A, and Martinez J (1991) Synthesis and biological activity of 2-phenylethyl ester analogues of C-terminal heptapeptide of cholecystokinin modified in Trp 30 region. *Int J Pept Protein Res* **38:**181–192.
Schwartz TW (1994) Locating ligand-binding sites in 7TM receptors by protein engineering. *Curr Opin Biotechnol* **5:**434–444.
Silvente-Poirot S, Escrieut C, and Wank SA (1998) Role of the extracellular domains of the cholecystokinin receptor in agonist binding. *Mol Pharmacol* **54:**364–371.
Strader CD, Fong TM, Tota MR, Underwood D, and Dixon RA (1994) Structure and function of G protein-coupled receptors. *Annu Rev Biochem* **63:**101–132.

Address correspondence to: Dr. Laurence J. Miller, Cancer Center, Mayo Clinic Scottsdale, 13400 East Shea Blvd., Scottsdale, AZ 85259. E-mail: miller@mayo.edu